Hindawi
Complexity
Volume 2021, Article ID 9915551, 9 pages
https://doi.org/10.1155/2021/9915551

Research Article

A New Scheme for Solving Multiorder Fractional Differential Equations Based on Müntz–Legendre Wavelets

Haifa Bin Jebreen and Fairouz Tchier

Department of Mathematics, College of Science, King Saud University, Riyadh, Saudi Arabia

Correspondence should be addressed to Haifa Bin Jebreen; hjebreen@ksu.edu.sa

Received 12 March 2021; Revised 4 April 2021; Accepted 20 July 2021; Published 31 July 2021

Academic Editor: Átila Madureira Bueno

In this study, we apply the pseudospectral method based on Müntz–Legendre wavelets to solve the multiorder fractional differential equations with Caputo fractional derivative. Using the operational matrix for the Caputo derivative operator and applying the Chebyshev and Legendre zeros, the problem is reduced to a system of linear algebraic equations. We illustrate the reliability, efficiency, and accuracy of the method by some numerical examples. We also compare the proposed method with others and show that the proposed method gives better results.

1. Introduction

This paper is dedicated to the numerical solution of the multiorder fractional differential equation with Caputo fractional derivative based on Müntz–Legendre wavelets. Let $\alpha \in \mathbb{R}_+$, $\mathbb{N} \ni n := [-\alpha]$, for $\alpha \notin \mathbb{N}$. Further, let $\alpha_j \in \mathbb{R}_+ (j = 1, \ldots, \sigma \in \mathbb{N})$ which satisfies

$$0 = \alpha_0 < \alpha_1 < \cdots < \alpha_\sigma < \alpha. \tag{1}$$

We aim to compute the approximate solution of the linear or nonlinear fractional differential equation

$$\begin{aligned} {}^c\mathscr{D}_0^{\alpha}(y)(x) &= f\left[x, y(x), {}^c\mathscr{D}_0^{\alpha_1}(y)(x), \ldots, {}^c\mathscr{D}_0^{\alpha_\sigma}(y)(x)\right], \quad x \in [0,1], \\ y^{(\eta)}(0) &= q_\eta, \quad q_\eta \in \mathbb{R}, \eta = 0, 1, \ldots, n-1, \end{aligned} \tag{2}$$

where ${}^c\mathscr{D}_0^{\alpha}$ is the Caputo fractional differential operator [1] and the function $f[x, y, y_1, \ldots, y_\sigma] \in C[0,1]$ with $y_1, \ldots, y_\sigma \in \mathscr{G}$ ($\mathscr{G} \subset \mathbb{C}$ is an open set) satisfies the Lipschitz condition

$$\left|f[x, y, y_1, \ldots, y_\sigma](x) - f[x, u, u_1, \ldots, u_\sigma](x)\right| \le \mathscr{L}_\sigma \sum_{j=0}^{\sigma} \left|y_j - u_j\right|, \quad y_j, u_j \in G, \tag{3}$$

where $\mathscr{L}_\sigma > 0$ is independent of x. We also assume for simplicity that

$$f_{\alpha_0,\ldots,\alpha_\sigma}[t,y] \coloneqq f\left[x, y(x), {}^c\mathscr{D}_0^{\alpha_1}(y)(x), \ldots, {}^c\mathscr{D}_0^{\alpha_\sigma}(y)(x)\right]. \tag{4}$$

The existence and uniqueness of L_1 solution of the multiorder fractional differential equation with the Riemann–Liouville and Caputo fractional derivatives under the assumption that $f(x,t) \in L_1[0,1]$ satisfies the Lipschitz condition with respect to the second variable are investigated by Kilbas et al. [1]. The previous investigation is based on converting equation (2) into the equivalent Volterra integral equation and then solving it. But in this study, we solve the problem directly.

There exist some numerical methods that solve the desired problem. Laksetani et al. [2] introduced an operational method using B-spline functions to solve the multiorder fractional differential equation

$$F\left(u(x), {}^cD_0^{\beta_1}, \ldots, {}^cD_0^{\beta_m}\right) = g(x), \quad \beta_i \in \mathbb{R}. \tag{5}$$

In this paper, the operational matrix of the Caputo fractional derivative has been constructed directly, and then using the collocation method, the problem is solved. In [3], the authors applied the collocation method to solve the fractional differential equation

$${}^cD^\alpha y(t) = f(t, y(t)), \quad \alpha \in (0,1]. \tag{6}$$

Their investigation is based on the collocation method using the Chebyshev–Gauss–Lobatto collocation points. The main advantage of this method is its superior accuracy. We can point out its exponential convergence too. But solving this problem is not a big challenge because it lacks multiorder fractional derivatives. Dehestani et al. [4] applied the fractional-Lucas optimization method to solve the multidimensional and multiorder fractional differential equation with Caputo fractional derivative. To this end, they used the operational matrix of fractional derivative for Lucas functions and reduced the problem into a linear or nonlinear system. The result shows the accuracy and efficiency of the method. A special type of equation (2) is considered by Bhrawy et al. [5] as

$${}^cD^\alpha y(t) + \gamma y(t) = f(t). \tag{7}$$

To solve this equation, they utilized the Laguerre tau technique. To this end, firstly fractional-order generalized Laguerre functions are introduced and Caputo fractional-order derivative is represented by these bases. In [6], after introducing the fractional-order Legendre functions and the operational matrix of Caputo derivative, the multiorder fractional differential equation is solved. For more details, we refer the readers to [7–10].

The fractional differential equations are applied to model various physical phenomena, such as heat conduction, viscoelasticity, dynamical behavior of quantum particles, and laxation and diffusion problems [11–16].

This paper is organized as follows. In Section 2, we introduce the Müntz–Legendre wavelets, and we construct the operational matrix of fractional integration and Caputo fractional derivative. In Section 3, the pseudospectral method is applied to solve the generalized Cauchy-type problems with Caputo fractional differentiation based on Müntz–Legendre wavelets, and then the error analysis is investigated. Section 4 is devoted to some numerical examples to illustrate the accuracy and efficiency of the proposed method.

2. Müntz–Legendre Wavelets

In the last decade, wavelets have been able to get a special place in numerical analysis and especially in the numerical solution of equations [17–22]. As you know, one of the ways to get wavelets is to use multiresolution analysis (MRA). MRA is a family of nested spaces that satisfies certain circumstances [23], namely,

$$\{0\} \subset \cdots \subset V_{-1} \subset V_0 \subset V_1 \subset \cdots \subset L^2(\Omega), \tag{8}$$

where Ω is a bounded interval or is equal to $\mathbb{R}$.

In this paper, we apply Müntz–Legendre wavelets to solve the multiorder fractional differential equations. To this end, we give a brief introduction to Müntz–Legendre wavelets. Assume that the space V_J ($J \in \mathbb{Z}^+ \cup \{0\}$) is spanned by a set of bases which are called multiscaling functions or mother wavelets, i.e.,

$$V_J = \operatorname{span}\left\{\psi_{J,b}^m : b \in \mathscr{B}, m \in \mathscr{M}\right\}, \tag{9}$$

where $\mathscr{B} \coloneqq \{0, 1, \ldots, 2^J - 1\}$ and $\mathscr{M} \coloneqq \{0, 1, \ldots, r-1\}$, $r \in \mathbb{N}$. The parameter r is called the multiplicity parameter, and J is the refinement level. In the following, we introduce the functions $\psi_{J,b}^m$.

Assume that $\lambda_k \coloneqq k\mu$ where μ is a real constant. Denote by $L_m(x)$ the Müntz–Legendre polynomials [24] which are defined on $\Omega \coloneqq [0,1]$ as

$$L_m(x) = \sum_{k=0}^{m} l_{k,m} x^{\lambda_k}, \quad x \in \Omega, \tag{10}$$

where the coefficient $l_{k,m}$ is defined by [24]

$$l_{k,m} \coloneqq \frac{\prod_{i=0}^{m-1}(\lambda_k + \lambda_i + 1)}{\prod_{i=0, i\neq k}^{m}(\lambda_k - \lambda_i)}. \tag{11}$$

Among the properties of these functions, we can mention their orthogonality. These polynomials form an orthogonal system that satisfies the following relation:

$$\langle L_{m'}(x), L_m(x)\rangle = \int_0^1 L_{m'}(x) L_m(x)\mathrm{d}x = \frac{\delta_{m',m}}{2\lambda_m + 1}, \quad m \geq m', \tag{12}$$

where $\delta_{m',m}$ is used for the Kronecker symbol and is given by

$$\delta_{m',m} \coloneqq \begin{cases} 1, & m = m', \\ 0, & m \geq m'. \end{cases} \tag{13}$$

Now we are ready to introduce the functions $\psi_{J,b}^m$. The Müntz–Legendre wavelets on the interval $[0,1]$ are defined as follows [24]:

$$\psi_{J,b}^{m}=\begin{cases}2^{J/2}\sqrt{2\lambda_m+1}\,L_m\left(2^J x-b\right), & \dfrac{b}{2^J}\le x\le\dfrac{b+1}{2^J},\\ 0, & \text{otherwise.}\end{cases} \tag{14}$$

Let $\mathscr{P}_J$ be an operator that projects any function $f(x)\in L^2[0,1]$ onto the subspace V_J as follows:

$$f(x)\approx\mathscr{P}_J(f)(x)=\sum_{b=0}^{2^J-1}\sum_{m=0}^{r-1}f_{b,m}\psi_{J,b}^{m}(x), \tag{15}$$

where the coefficients $\{f_{b,m}\}$ are evaluated by

$$f_{b,m}=\langle f,\psi_{J,b}^{m}\rangle=\int_0^1 f(x)\psi_{J,b}^{m}(x)\mathrm{d}x. \tag{16}$$

Let F and $\Psi(x)$ be vectors of dimension $N=2^J r$ whose $(br+m+1)$-th element is $f_{b,m}$ and $\psi_{J,b}^{m}(x)$, respectively. Hence, it follows from equation (15) that

$$f(x)\approx\mathscr{P}_J(f)(x)=F^T\Psi(x), \tag{17}$$

where the superscript T is used for the matrix transpose.

It follows from [24] that there are some error estimates in the sense of Sobolev norms.

Lemma 1 (see [24]). *Let $n\ge 0$ and $r>n$. If $f\in H^n[0,1]$, then*

$$\left\|f-\mathscr{P}_J(f)\right\|_{L_2(0,1)}\le c(r-1)^{-n}\left(2^{J-1}\right)^{-n}\left\|f^{(n)}\right\|_{L_2(0,1)}, \tag{18}$$

and for $s\ge 1$, we have

$$\left\|f-\mathscr{P}_J(f)\right\|_{H^s(0,1)}\le c(r-1)^{2s-(1/2)-n}\left(2^{J-1}\right)^{s-n}\left\|f^{(n)}\right\|_{L_2(0,1)}, \tag{19}$$

where $H^n(0,1)$ is the Sobolev space and

$$\|f\|_{H^n(0,1)}=\left(\sum_{j=0}^{n}\left\|f^{(j)}\right\|_{L_2(0,1)}^2\right)^{1/2}. \tag{20}$$

2.1. Representation of the Caputo Fractional Derivative Operator in Müntz–Legendre Wavelets. Recall that the Riemann–Liouville fractional integral operator $\mathscr{I}_0^{\alpha}$ $(\alpha\in\mathbb{R}^+)$ is determined by

$$\mathscr{I}_a^{\alpha}f(x):=\frac{1}{\Gamma(\alpha)}\int_a^x(x-s)^{\alpha-1}f(s)\mathrm{d}s,\quad x\in[a,b]. \tag{21}$$

Note that if $f\in L_1[a,b]$, then the function $\mathscr{I}_a^{\alpha}f\in L_1[a,b]$. We know that there is an operator that satisfies the relation

$${}^{RL}\mathscr{D}_a^{\alpha}=\mathscr{D}^n\mathscr{I}_a^{n-\alpha}, \tag{22}$$

where $\mathscr{D}:=(\mathrm{d}/\mathrm{d}x)$ and ${}^{RL}\mathscr{D}_a^{\alpha}$ is called the Riemann–Liouville fractional derivative operator. There is also another fractional derivative operator that satisfies the relation ${}^{c}\mathscr{D}_a^{\alpha}f(x):=\mathscr{I}_a^{n-\alpha}\mathscr{D}^n(f)(x)$ and is called the Caputo fractional derivative.

In this section, we would like to represent the Caputo fractional derivative operator in Müntz–Legendre wavelets. To this end, we first construct the operational matrix for fractional integral operator $\mathscr{I}_0^{\alpha}$. Then, applying the operational matrix of derivative D for Müntz–Legendre wavelets [25] and relation ${}^{c}\mathscr{D}_a^{\alpha}f(x):=\mathscr{I}_a^{n-\alpha}\mathscr{D}^n(f)(x)$, we can find the operational matrix of fractional derivative for Müntz–Legendre wavelets.

Applying the projection operator $\mathscr{P}$, the fractional integral operator $\mathscr{I}_0^{\alpha}$ acting on the vector function $\Psi(x)$ can be approximated by

$$\mathscr{P}\left(\mathscr{I}_0^{\alpha}\right)(\Psi(x))=I_{\alpha}(x)\Psi(x),\quad \alpha\in(0,1), \tag{23}$$

where $I_{\alpha}(x)$ is the operational matrix of integral for the Müntz–Legendre wavelets.

To facilitate the evaluation of the operational matrix elements of fractional integration for the Müntz–Legendre wavelets, it is necessary to introduce the piecewise fractional-order Taylor functions. For a fixed $J\in\mathbb{Z}^+\cup\{0\}$, these functions are constructed as

$$\phi_{J,b}^{m}=\begin{cases}t^{\lambda_m}, & \dfrac{b}{2^J}\le x\le\dfrac{b+1}{2^J},\\ 0, & \text{otherwise,}\end{cases} \tag{24}$$

$$b\in\mathscr{B},m\in\mathscr{M}.$$

Let $\Phi(x)$ be a vector of dimension N whose $(br+m+1)$-th element is $\phi_{J,b}^{m}(x)$.

To derive matrix $I_{\alpha}(x)$, we first introduce a matrix of dimension $N\times N$ that is used to transfer the Müntz–Legendre wavelets $\Psi(x)$ to the piecewise fractional-order Taylor functions $\Phi(x)$. Assume that there is a matrix of dimension $N\times N$ such that

$$\Psi(x)=T^{-1}\Phi(x), \tag{25}$$

where T_J^{-1} stands for the inverse of the matrix T. The matrix T is called the transformation matrix whose (i,j)-th element is evaluated by

$$T_{i,j}=\langle\Phi_i(x),\Psi_j(x)\rangle=\int_0^1\Phi_i(x)\Psi_j(x)\mathrm{d}x,\quad i,j=1,\ldots,N. \tag{26}$$

Let Λ be a vector of dimension r whose i-th element is x^{λ_i}, and thus it follows from equation (24) that

$$\Phi(x)=[\Lambda,\ldots,\Lambda]^T. \tag{27}$$

It is easy to verify that the Riemann–Liouville fractional integration of the power functions x^{κ} is equal to power functions of the same form, i.e.,

$$\mathscr{I}_0^{\alpha}\left(x^{\kappa}\right)=\frac{\Gamma(\kappa+1)}{\Gamma(\kappa+\alpha+1)}x^{\kappa+\alpha}. \tag{28}$$

This gives rise to find the i-th element of $\mathscr{I}_0^{\alpha}(\Phi)(x)$, via

$$\mathscr{I}_0^{\alpha}(\Phi_i)(x) = \frac{\Gamma(\lambda_i+1)}{\Gamma(\lambda_i+\alpha+1)}x^{\lambda_i+\alpha}. \tag{29}$$

Thus, there exists a diagonal matrix $I_{\Phi,\alpha}(x)$ of dimension $N \times N$ such that

$$\mathscr{I}_0^{\alpha}(\Phi)(x) = I_{\Phi,\alpha}(x)\Phi(x). \tag{30}$$

The matrix $I_{\Phi,\alpha}(x)$ elements are obtain as follows:

$$I_{\Phi,\alpha}(x) = \operatorname{diag}\left[I_{T,\alpha}(x), \ldots, I_{T,\alpha}(x)\right], \tag{31}$$

where $I_{T,\alpha}(x) \coloneqq x^{\alpha}G\,(\mathscr{I}_0^{\alpha}(\Lambda)(x) = I_{T,\alpha}(x)\Lambda(x))$ and G is a diagonal matrix of the form

$$(G)_{i,i} = \frac{\Gamma(\lambda_i+1)}{\Gamma(\lambda_i+\alpha+1)}. \tag{32}$$

To derive the operational matrix of integral for the Müntz–Legendre wavelets, it follows from equation (25) that

$$\begin{aligned}\mathscr{P}\left(\mathscr{I}_0^{\alpha}\right)(\Psi(x)) &= \mathscr{P}\left(\mathscr{I}_0^{\alpha}\right)\left(T^{-1}\Phi(x)\right)\\ &= T^{-1}I_{\Phi,\alpha}(x)\Phi(x)\\ &= T^{-1}I_{\Phi,\alpha}(x)T\Psi(x).\end{aligned} \tag{33}$$

This gives rise to

$$I_{\alpha}(x) \coloneqq T^{-1}I_{\Phi,\alpha}(x)T. \tag{34}$$

Now using ${}^{c}\mathscr{D}_a^{\alpha} \coloneqq \mathscr{I}_a^{n-\alpha}\mathscr{D}^n$, we can introduce the operational matrix for the Caputo fractional derivative

$$D_{\alpha}(x) \coloneqq D^n I_{n-\alpha}(x). \tag{35}$$

3. Pseudospectral Method

To derive the numerical solution of equation (2), the approximate solution can be approximated by Müntz–Legendre wavelets as follows:

$$y \approx \mathscr{P}(y)(x) = Y^T\Psi(x), \tag{36}$$

where Y is a vector of dimension N that should be determined. A similar expression is valid for $F_{\alpha_0,\ldots,\alpha_\sigma}[x, \mathscr{P}(y)(x)] \in C_{\gamma}([0,1])$ where $C_{\gamma}([0,1])$ is the space of functions that satisfies $(x-a)^{\gamma}f(x) \in C([0,1])$ for $0 \le \gamma < 1$.

$$\mathscr{P}\left(f_{\alpha_0,\ldots,\alpha_\sigma}[x, \mathscr{P}(y)(x)]\right)(x) = F^T\Psi(x). \tag{37}$$

To compute the elements of matrix F, let $y_J = \mathscr{P}(y)$; then, using ${}^{c}\mathscr{D}_a^{\alpha} \coloneqq \mathscr{I}_a^{n-\alpha}\mathscr{D}^n$,

$$\begin{aligned}\mathscr{P}\left(f_{\alpha_0,\ldots,\alpha_\sigma}\left[x, y_J(x)\right]\right)(x) &= f\left[x, y_J(x), {}^{c}\mathscr{D}_a^{\alpha_1}\left(y_J\right)(x), \ldots, {}^{c}\mathscr{D}_a^{\alpha_\sigma}\left(y_J\right)(x)\right]\\ &= f\left[x, y_J(x), \mathscr{I}_0^{n_1-\alpha_1}\mathscr{D}^{n_1}\left(y_J\right)(x), \ldots, \mathscr{I}_0^{n_\sigma-\alpha_\sigma}\mathscr{D}^{n_\sigma}\left(y_J\right)(x)\right],\\ \mathscr{I}_0^{n_j-\alpha_j}\mathscr{D}^{n_j}\left(y_J\right)(x) &\coloneqq Y^T\mathscr{I}_0^{n_j-\alpha_j}\mathscr{D}^{n_j}(\Psi)(x) = Y^T\mathscr{I}_0^{n_j-\alpha_j}\mathscr{D}^{n_j}(\Psi)(x)\\ &= Y^T\mathscr{D}^{n_j}I_{n_j-\alpha_j}(x)\Psi(x), \quad j = 1, \ldots, \sigma.\end{aligned} \tag{38}$$

It follows from equations (36) and (38) that we can compute the residual in approximating equation (2) as follows:

$$r_J(x) = \left(D_{\alpha}Y^T - F^T\right)(x)\Psi(x). \tag{39}$$

We aim to reduce the residual to zero. One of the available methods is to use the pseudospectral method such that $r_J(x_i) = 0$ where x_i are the collocation points. In this paper, we use the shifted Legendre and Chebyshev polynomial zeros. This gives rise to a system of linear or nonlinear algebraic equations that should be solved to find the unknown coefficients Y. To apply the initial conditions (2), we replace the first n equations of the obtained system of the pseudospectral method with them.

$$\left[r_J(x_i)\right]_{\eta} \coloneqq Y^T\mathscr{D}^{\eta}\Psi(0) - q_{\eta}, \quad \eta = 0, \ldots, n-1. \tag{40}$$

3.1. Convergence Analysis. It follows from [1] that the fractional integration operators $\mathscr{I}_0^{\alpha}$ is bounded in $L_p[0,1]$ (see [1] Lemma 1(a))

$$\begin{aligned}\left\|\mathscr{I}_0^{\alpha}y\right\|_{L_p(0,1)} &\le \mathscr{C}_{\alpha}\|y\|_{L_p(0,1)},\\ \mathscr{C}_{\alpha} &= \frac{1}{\Gamma(\alpha+1)}.\end{aligned} \tag{41}$$

Also there is an optimal error estimate in term of error between the Müntz–Legendre polynomials derivative $\mathscr{D}y$ and the exact derivative $\mathscr{P}(\mathscr{D}y)$, via

$$\|\mathscr{D}y - \mathscr{P}(\mathscr{D}y)\|_{L_2(0,1)} \le C_D(r-1)^{1-n}|y|_{H^{n,r-1}(0,1)}, \tag{42}$$

where C_D is a constant and

$$|g|^2_{H^{n,r-1}(0,1)} = \sum_{l=\min\{n,r-1\}}^{r-1}\left\|g^{(l)}(t)\right\|^2_{L^2(0,1)} \tag{43}$$

is a seminorm.

Theorem 1. *Let $n = [-\alpha]$ and $\alpha \in \mathbb{R}_+$. Assume that $f_{\alpha_0,\ldots,\alpha_\sigma}[t,y] \in H^n[0,1]$ and satisfies the Lipschitz condition (3). Also, assume that y and y_J are the exact and the approximate solutions (39) of equation (2), respectively.*

If y is a sufficiently smooth function, then the overall error

$$e(x) = {}^{c}\mathscr{D}_0^{\alpha}(y)(x) - \mathscr{P}\left({}^{c}\mathscr{D}_0^{\alpha}(y)\right)(x) - f_{\alpha_0,\ldots,\alpha_\sigma}[t,y] + \mathscr{P}\left(f_{\alpha_0,\ldots,\alpha_\sigma}\left[t,y_J\right]\right) \tag{44}$$

satisfies

$$\|e(x)\|_{L_2(0,1)} \longrightarrow 0, \quad \text{as } r \longrightarrow \infty, \text{ or } J \longrightarrow \infty. \tag{45}$$

Proof. If $f_{\alpha_0,\ldots,\alpha_\sigma}[t,y] \in H^n[0,1]$, then by Lemma 1, we can write

$$\left\|f_{\alpha_0,\ldots,\alpha_\sigma}\left[t,y_J\right] - \mathscr{P}_J\left(f_{\alpha_0,\ldots,\alpha_\sigma}\left[t,y_J\right]\right)\right\|_{L_2(0,1)} \le c_1(r-1)^{-n}\left(2^{J-1}\right)^{-n}\left\|f^{(n)}_{\alpha_0,\ldots,\alpha_\sigma}\left[t,y_J\right]\right\|_{L_2(0,1)}. \tag{46}$$

Using the Lipschitz conditions (3) and (41), we can write the following bound:

$$\begin{aligned}\left\|f_{\alpha_0,\ldots,\alpha_\sigma}[t,y] - f_{\alpha_0,\ldots,\alpha_\sigma}\left[t,y_J\right]\right\|_{L_2(0,1)} &\le \left|\mathscr{L}_\sigma\right|\left\|\sum_{j=0}^{\sigma} {}^{c}\mathscr{D}_0^{\alpha_j}\left(y - y_J\right)\right\|_{L_2(0,1)}\\ &= \left|\mathscr{L}_\sigma\right|\left\|\sum_{j=0}^{\sigma} \mathscr{I}_0^{n_j-\alpha_j}\mathscr{D}^{n_j}\left(y - y_J\right)\right\|_{L_2(0,1)}\\ &\le \left|\mathscr{L}_\sigma\right|\sum_{j=0}^{\sigma}\mathscr{C}_{n_j-\alpha_j}\left\|\mathscr{D}^{n_j}\left(y - y_J\right)\right\|_{L_2(0,1)}.\end{aligned} \tag{47}$$

Now, applying equation (41) and Theorem 2 [24], we have

$$\begin{aligned}\left\|f_{\alpha_0,\ldots,\alpha_\sigma}[t,y] - f_{\alpha_0,\ldots,\alpha_\sigma}\left[t,y_J\right]\right\|_{L_2(0,1)} &\le \left|\mathscr{L}_\sigma\right|\sum_{j=0}^{\sigma}\mathscr{C}_{n_j-\alpha_j}C_{D^{n_j}}(r-1)^{1-n}\left|y^{\left(n_j-1\right)}\right|_{H^{n,r-1}(0,1)}\\ &\le \left|\mathscr{L}_\sigma\right|\sum_{j=0}^{\sigma}\mathscr{C}_{n_j-\alpha_j}C_{D^{n_j}}(r-1)^{1-n}\left(2^{J-1}\right)^{-n}\left\|y^{\left(n+n_j-1\right)}\right\|_{L_2(0,1)}.\end{aligned} \tag{48}$$

Also, using Lemma 1 and equation (41), we have

$$\begin{aligned}\left\|{}^{c}\mathscr{D}_0^{\alpha}(y)(x) - \mathscr{P}\left({}^{c}\mathscr{D}_0^{\alpha}(y)\right)(x)\right\|_{L_2(0,1)} &\le c_2(r-1)^{-n}\left(2^{J-1}\right)^{-n}\left\|{}^{c}\mathscr{D}_0^{\alpha}y\right\|_{L_2(0,1)}\\ &= \le c_2(r-1)^{-n}\left(2^{J-1}\right)^{-n}\left\|\mathscr{I}_0^{n-\alpha}\mathscr{D}^{n}(y)\right\|_{L_2(0,1)}\\ &\le C_{n-\alpha}c_2(r-1)^{-n}\left(2^{J-1}\right)^{-n}\left\|y^{n}\right\|_{L_2(0,1)}.\end{aligned} \tag{49}$$

Subtracting equation (2) from equation (39), one can write

$$e(x) = {}^{c}\mathscr{D}_0^{\alpha}(y)(x) - \mathscr{P}\left({}^{c}\mathscr{D}_0^{\alpha}(y)\right)(x) - f_{\alpha_0,\ldots,\alpha_\sigma}[t,y] + \mathscr{P}\left(f_{\alpha_0,\ldots,\alpha_\sigma}\left[t,y_J\right]\right) + f_{\alpha_0,\ldots,\alpha_\sigma}\left[t,y_J\right] - f_{\alpha_0,\ldots,\alpha_\sigma}\left[t,y_J\right]. \tag{50}$$

Taking norms from both sides of equation (50) and using equations (46)–(49), we end up with

$$\begin{aligned}\|e(x)\|_{L_2(0,1)} \le{}& \left\|{}^c\mathscr{D}_0^{\alpha}(y)(x) - \mathscr{P}\left({}^c\mathscr{D}_0^{\alpha}(y)\right)(x)\right\|_{L_2(0,1)} + \left\|f_{\alpha_0,\ldots,\alpha_\sigma}[t,y] - f_{\alpha_0,\ldots,\alpha_\sigma}[t,y_J]\right\|_{L_2(0,1)}\\ &+ \left\|f_{\alpha_0,\ldots,\alpha_\sigma}[t,y_J] - \mathscr{P}\left(f_{\alpha_0,\ldots,\alpha_\sigma}[t,y_J]\right)\right\|_{L_2(0,1)}\\ \le{}& C_{n-\alpha}c_2(r-1)^{-n}\left(2^{J-1}\right)^{-n}\left\|y^n\right\|_{L_2(0,1)}\\ &+ \left|\mathscr{L}_\sigma\right|\sum_{j=0}^{\sigma}\mathscr{C}_{n_j-\alpha_j}C_{D^{n_j}}(r-1)^{1-n}\left(2^{J-1}\right)^{-n}\left\|y^{(n+n_j-1)}\right\|_{L_2(0,1)}\\ &+ c_1(r-1)^{-n}\left(2^{J-1}\right)^{-n}\left\|f^{(n)}_{\alpha_0,\ldots,\alpha_\sigma}[t,y_J]\right\|_{L_2(0,1)}.\end{aligned} \tag{51}$$

Suppose that $C_1 := \max\{\mathscr{C}_{n_j-\alpha_j}C_{D^{n_j}}\}$ $(j=0,\ldots,\sigma)$ and $C := \max\{C_{n-\alpha}c_2, C_1, c_1\}$; then, we can obtain the following from equation (51):

$$\|e(x)\|_{L_2(0,1)} \le C(r-1)^{-n}\left(2^{J-1}\right)^{-n}\left(\left\|y^n\right\|_{L_2(0,1)} + \left|\mathscr{L}_\sigma\right|\sum_{j=0}^{\sigma}\left\|y^{(n+n_j-1)}\right\|_{L_2(0,1)} + \left\|f^{(n)}_{\alpha_0,\ldots,\alpha_\sigma}[t,y_J]\right\|_{L_2(0,1)}\right). \tag{52}$$

It is easy to show that $\|e(x)\|_{L_2(0,1)} \longrightarrow 0$ as $r \longrightarrow \infty$ or $J \longrightarrow \infty$. □

4. Numerical Implementation

In this section, we reported the numerical results for some examples to show the accuracy and efficiency of the method. To this end, we have performed all numerical computations in Maple and Matlab simultaneously. Wherever collocation nodes have not been reported, we have used Legendre nodes.

Example 1. Let us dedicate the first example to the following one.

$$\begin{aligned}&{}^c\mathscr{D}_0^{\alpha}(y)(x) + {}^c\mathscr{D}_0^{\alpha_1}(y)(x) + [y(x)]^2 = \left(x^2-x\right)^2 + \frac{2x^{2-\alpha}}{\Gamma(3-\alpha)} + \frac{2x^{2-\alpha_1}}{\Gamma(3-\alpha_1)} - \frac{2x^{1-\alpha_1}}{\Gamma(2-\alpha_1)},\\ &y(0)=0, y'(0)=-1.\end{aligned} \tag{53}$$

The exact solution is reported in [4] as follows:

$$y(x) = x^2 - x. \tag{54}$$

To show the ability and efficiency of the proposed method, Tables 1 and 2 are reported. The absolute error for proposed method is compared with the fractional-Lucas optimization method [4] and Chebyshev wavelet method [26] in Table 1. The results illustrate that the proposed method is flexible against other methods and gives a better approximation. We show L_2–error, L_∞–error, and CPU time for different values of α and α_1 taking $\mu = 0.5$ in Table 2.

Example 2. The second example is dedicated to the following equation:

$$\begin{aligned}&{}^c\mathscr{D}_0^{\alpha}(y)(x) + [y(x)]^2 = x + \left(\frac{x^{\alpha+1}}{\Gamma(\alpha+2)}\right)^2,\\ &y(0) = 0 y'(0) = -1.\end{aligned} \tag{55}$$

The exact solution is reported in [5] as follows:

$$y(x) = \frac{x^{\alpha+1}}{\Gamma(\alpha+2)}, \quad 0 < \alpha \le 2. \tag{56}$$

In Table 3, we compare the maximum of absolute value error of our method with fractional-order generalized Laguerre functions (FGLFs) [5]. In this example, we set the value of μ equal to α. L^2–errors taking different vales for r and absolute value of error for different values of α are plotted in Figure 1.

Table 1: Comparison of the absolute error for Example 1.

x	Our method		Fractional-Lucas optimization method [4] ($\mathfrak{m} = 2$)	Chebyshev wavelet method [26] ($M = 6, k = 4$)
	Chebyshev nodes ($r = 5, J = 1, \mu = 0.5$)	Legendre nodes ($r = 5, J = 1, \mu = 0.5$)		
0.1	1.3620×10^{-49}	2.0240×10^{-49}	2.8022×10^{-17}	8.8658×10^{-6}
0.2	6.2780×10^{-49}	5.2750×10^{-49}	1.1208×10^{-14}	8.5359×10^{-6}
0.3	1.3344×10^{-48}	9.4020×10^{-49}	2.5219×10^{-14}	8.1318×10^{-6}
0.4	2.1909×10^{-48}	1.4212×10^{-48}	4.4835×10^{-14}	7.6897×10^{-6}
0.5	3.1020×10^{-48}	1.9086×10^{-48}	7.0055×10^{-14}	7.1843×10^{-6}
0.6	4.0646×10^{-48}	2.4139×10^{-48}	1.0087×10^{-13}	6.7665×10^{-6}
0.7	4.9381×10^{-48}	2.8187×10^{-48}	1.3730×10^{-13}	6.3058×10^{-6}
0.8	5.8985×10^{-48}	3.3089×10^{-48}	1.7934×10^{-13}	5.8497×10^{-6}
0.9	6.8068×10^{-48}	3.7540×10^{-48}	2.2697×10^{-13}	5.4018×10^{-6}

Table 2: L_2–error, L_∞–error, and CPU time taking different values for α and α_1 for Example 1.

	$\alpha = 1.75$			$\alpha = 1.80$		
	$\alpha_1 = 0.2$	$\alpha_1 = 0.5$	$\alpha_1 = 0.8$	$\alpha_1 = 0.2$	$\alpha_1 = 0.5$	$\alpha_1 = 0.8$
L_2–error	5.52×10^{-49}	2.41×10^{-48}	2.76×10^{-48}	1.35×10^{-47}	1.16×10^{-47}	1.33×10^{-47}
L_∞–error	8.92×10^{-49}	3.66×10^{-48}	4.24×10^{-48}	2.10×10^{-47}	1.78×10^{-47}	2.07×10^{-47}
CPU time	0.906	0.969	1.031	0.953	0.985	0.968

Table 3: The maximum of absolute value error taking different values for r and α for Example 2.

	$r = 8$			$r = 12$		
	$\alpha = 0.5$	$\alpha = 0.7$	$\alpha = 0.8$	$\alpha = 0.5$	$\alpha = 0.7$	$\alpha = 0.8$
Our method	8.31×10^{-46}	9.72×10^{-5}	1.56×10^{-4}	7.55×10^{-46}	1.89×10^{-5}	3.32×10^{-5}
FGLFs [5]	1.42×10^{-14}	4.28×10^{-3}	6.08×10^{-3}	1.42×10^{-14}	1.74×10^{-3}	1.87×10^{-3}

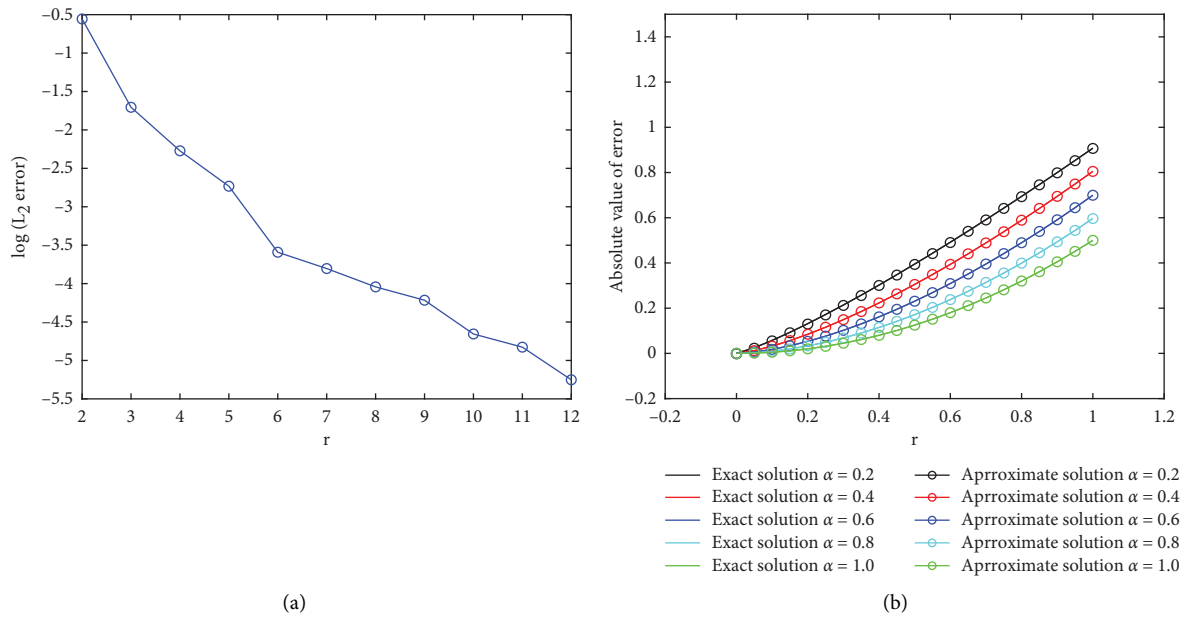

(a) (b)

Figure 1: Plot of L^2–errors taking different vales for r (a) and absolute value of error for different values of α (b) for Example 2.

Example 3. We dedicated this example to the Bagley–Torvik equation [27, 28]:

$$\mathscr{D}^2 y(x) + {}^c\mathscr{D}_0^{3/2}(y)(x) + y(x) = 1 + x, \quad y(0) = 1, y'(0) = 1. \tag{57}$$

The exact solution can be found in [27, 28], which is $y(x) = x + 1$.

In Figure 2, we plot the exact solution along with the approximate solution. Also, in this figure, the absolute value of error is reported for $\mu = 0.5$, $r = 3$, and $J = 1$. In Table 4, we compare the proposed method with the Bessel

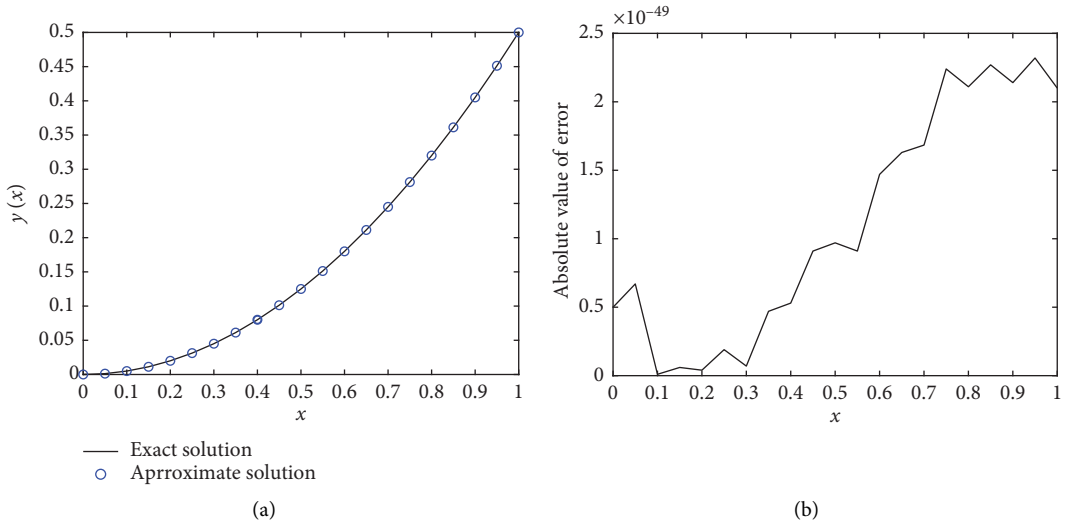

(a) (b)

Figure 2: Plot of the exact solution along with the approximate solution (a) and absolute value of error (b) for Example 3.

Table 4: Comparison of the absolute error for Example 3.

	Our method	Bessel collocation method [28]	
	$r = 3$	$N = 6$	$N = 9$
0.1	1.0×10^{-51}	6.1919×10^{-16}	9.3742×10^{-16}
0.2	4.0×10^{-51}	1.0292×10^{-15}	3.9634×10^{-15}
0.3	7.0×10^{-51}	1.4779×10^{-15}	4.2834×10^{-15}
0.4	5.3×10^{-50}	1.9697×10^{-15}	3.2975×10^{-15}
0.5	9.7×10^{-50}	2.4941×10^{-15}	2.0455×10^{-15}
0.6	1.47×10^{-49}	3.0365×10^{-15}	1.0277×10^{-15}
0.7	1.68×10^{-49}	3.5805×10^{-15}	3.4773×10^{-16}
0.8	2.11×10^{-49}	4.1090×10^{-15}	6.9289×10^{-17}
0.9	2.14×10^{-49}	4.6047×10^{-15}	2.3947×10^{-16}
1.0	2.10×10^{-49}	5.0500×10^{-15}	1.2006×10^{-16}

collocation method [28]. We observe that our method gives a better result than [28]. In this example, we put $\mu = 0.5$.

5. Conclusion

In this paper, we apply the pseudospectral method based on Müntz–Legendre wavelets to solve the multiorder fractional differential equations with Caputo fractional derivative. To this end, we represent the Caputo fractional derivative operator in the Müntz–Legendre wavelets. The results illustrate that by selecting the proper value for μ, the proposed method gives better results than others. The most important advantage of this method over other methods is its flexibility and ease of use. In most cases, the approximate solution is very close to the exact solution and we can almost say that the exact solution is obtained.

Data Availability

The data used to support this study are included within this article.

Conflicts of Interest

The authors declare that they have no conflicts of interest.

Authors' Contributions

All authors contributed equally and significantly in writing this paper. All authors read and approved the final manuscript.

Acknowledgments

The authors extend their appreciation to the Deanship of Scientific Research at King Saud University for funding this work through Research Group no. RG-1441-326.

References

[1] A. Kilbas, H. M. Srivastava, and J. J. Trujillo, *Theory and Applications of Fractional Differential Equations*, Elsevier, Amsterdam, Netherlands, 2006.

[2] M. Lakestani, M. Dehghan, and S. Irandoust-Pakchin, "The construction of operational matrix of fractional derivatives using B-spline functions," *Communications in Nonlinear Science and Numerical Simulation*, vol. 17, no. 3, pp. 1149–1162, 2012.

[3] S. Esmaeili, M. Luchko, and Y. Luchkob, "Numerical solution of fractional differential equations with a collocation method based on Müntz polynomials," *Computers & Mathematics with Applications*, vol. 62, no. 3, pp. 918–929, 2011.

[4] H. Dehestani, Y. Ordokhani, and M. Razzaghi, "Fractional-lucas optimization method for evaluating the approximate solution of the multi-dimensional fractional differential equations," *Engineering with Computers*, pp. 1–17, 2020.

[5] A. Bhrawy, Y. Alhamed, D. Baleanu, and A. Al-Zahrani, "New spectral techniques for systems of fractional differential equations using fractional-order generalized Laguerre orthogonal functions," *Fractional Calculus and Applied Analysis*, vol. 17, no. 4, pp. 1137–1157, 2014.

[6] S. Kazem, S. Abbasbandy, and S. Kumar, "Fractional-order Legendre functions for solving fractional-order differential equations," *Applied Mathematical Modelling*, vol. 37, no. 7, pp. 5498–5510, 2013.

[7] I. Hashim, O. Abdulaziz, and S. Momani, "Homotopy analysis method for fractional IVPs," *Communications in Nonlinear Science and Numerical Simulation*, vol. 14, no. 3, pp. 674–684, 2009.

[8] P. Kumar and O. P. Agrawal, "An approximate method for numerical solution of fractional differential equations," *Signal Processing*, vol. 86, no. 10, pp. 2602–2610, 2006.

[9] Z. Odibat and S. Momani, "An algorithm for the numerical solution of differential equations of fractional order," *Journal of Applied Mathematics and Informatics*, vol. 26, pp. 15–27, 2008.

[10] A. Saadatmandi and M. Dehghan, "A new operational matrix for solving fractional-order differential equations," *Computers & Mathematics with Applications*, vol. 59, no. 3, pp. 1326–1336, 2010.

[11] F. Ben Adda and J. Cresson, "Fractional differential equations and the Schrödinger equation," *Applied Mathematics and Computation*, vol. 161, no. 1, pp. 323–345, 2005.

[12] J. F. Douglas, "Some applications of fractional calculus to polymer science," *Advances in Chemical Physics*, vol. 102, pp. 121–191, John Wiley & Sons, Inc, Hoboken, NJ, USA, 2007.

[13] M. Inc, M. N. Khan, I. Ahmad, S.-W. Yao, H. Ahmad, and P. Thounthong, "Analysing time-fractional exotic options via efficient local meshless method," *Results in Physics*, vol. 19, Article ID 103385, 2020.

[14] J.-F. Li, I. Ahmad, H. Ahmad et al., "Numerical solution of two-term time-fractional PDE models arising in mathematical physics using local meshless method," *Open Physics*, vol. 18, no. 1, pp. 1063–1072, 2020.

[15] S. Qureshi, A. Yusuf, A. A. Shaikh, and M. Inc, "Transmission dynamics of varicella zoster virus modeled by classical and novel fractional operators using real statistical data," *Physica A: Statistical Mechanics and its Applications*, vol. 534, Article ID 122149, 2019.

[16] L. Zada, R. Nawaz, M. Ayaz, H. Ahmad, H. Alrabaiah, and Y. M. Chu, "New algorithm for the approximate solution of generalized seventh order Korteweg-Devries equation arising in shallow water waves," *Results in Physics*, vol. 20, Article ID 103744, 2021.

[17] B. K. Alpert, "A class of bases in $L2$ for the sparse representation of integral operators," *SIAM Journal on Mathematical Analysis*, vol. 24, no. 1, pp. 246–262, 1993.

[18] B. Alpert, G. Beylkin, R. Coifman, and V. Rokhlin, "Wavelet-like bases for the fast solution of second-kind integral equations," *SIAM Journal on Scientific Computing*, vol. 14, no. 1, pp. 159–184, 1993.

[19] B. Alpert, G. Beylkin, D. Gines, and L. Vozovoi, "Adaptive solution of partial differential equations in multiwavelet bases," *Journal of Computational Physics*, vol. 182, no. 1, pp. 149–190, 2002.

[20] B. N. Saray, "Abel's integral operator: sparse representation based on multiwavelets," *Bit Numerical Mathematics*, vol. 61, no. 1, 2021.

[21] M. Shahriari, B. N. Saray, M. Lakestani, and J. Manafian, "Numerical treatment of the Benjamin-Bona-Mahony equation using Alpert multiwavelets," *The European Physical Journal Plus*, vol. 133, no. 5, pp. 1–12, 2018.

[22] S. H. Seyedi, B. Nemati Saray, and A. Ramazani, "On the multiscale simulation of squeezing nanofluid flow by a highprecision scheme," *Powder Technology*, vol. 340, pp. 264–273, 2018.

[23] S. G. Mallat, *A Wavelet Tour of Signal Processing*, Academic Press, Cambridge, MA, USA, 1999.

[24] P. Rahimkhani, Y. Ordokhani, and E. Babolian, "Müntz-Legendre wavelet operational matrix of fractional-order integration and its applications for solving the fractional pantograph differential equations," *Numerical Algorithms*, vol. 77, no. 4, pp. 1283–1305, 2018.

[25] S. Sabermahani and Y. Ordokhani, "A new operational matrix of Müntz-Legendre polynomials and Petrov-Galerkin method for solving fractional Volterra-Fredholm integrodifferential equations," *Computational Methods for Differential Equations*, vol. 8, no. 3, pp. 408–423, 2020.

[26] L. Yuanlu, "Solving a nonlinear fractional differential equation using Chebyshev wavelets," *Communications in Nonlinear Science and Numerical Simulation*, vol. 15, no. 9, pp. 2284–2292, 2010.

[27] V. S. Krishnasamy and M. Razzaghi, "The numerical solution of the bagley–torvik equation with fractional taylor method," *Journal of Computational and Nonlinear Dynamics*, vol. 11, no. 5, Article ID 051010, 2016.

[28] S. Yüzbaşi, "Numerical solution of the Bagley-Torvik equation by the bessel collocation method," *Mathematical Methods in Applied Sciences*, vol. 36, no. 3, pp. 300–312, 2013.